Electroless Copper Bonding with Local Suppression for Void-Free Chip-to-Package Connections

Hyo-Chol Koo,* **Rajarshi Saha, and Paul A. Kohl****,z

Department of Chemical and Biomolecular Engineering, Georgia Institute of Technology, Atlanta, Georgia 30332-0100, USA

The effect of bis-(3-sulfopropyl)-disulfide (SPS) on the void-free electroless pillar-to-pillar bonding process has been investigated. Two dome-shaped Cu pillars were joined using electroless copper deposition with the addition of a suppressor to achieve solid, compliant Cu-to-Cu bonding without high temperature or pressure. SPS was added to the electroless copper plating bath which has strong suppression to the electroless plating in order to avoid the creation of an unbonded seam between the two Cu structures being bonded. The bath suppresses the deposition of copper near the entrance of the gap between the two pillars, while allowing high deposition rate in the geometrically restricted area between the copper structures being bonded. This phenomenon is due to diffusion of SPS through the narrow gap between the pillars being bonded. At adequate concentration of SPS, the two pillars were successfully joined without any remaining seam between the joined structures, by growth of copper from the center of the gap to the outside.
© 2012 The Electrochemical Society. [DOI: 10.1149/2.029206jes] All rights reserved.

Direct copper-to-copper bonding is a path to overcoming issues related to current solder-based flip-chip bonding technologies. Copper has excellent thermal and electrical conductivity, thermal stability, and superior electromigration resistance compared to solder.[1] Direct copper-to-copper fusion requires aggressive conditions, such as one or more of the following: elevated temperature, high pressure, vacuum conditions, and atomically clean surfaces.[2–8] Further, solder provides a fillet of material between the two components being joined so that non-planar surfaces can be joined without having to be made flat or co-planar. Excessive force would have to be applied to copper pillars, or other I/O structures if direct copper-copper bonding were used to join components.

The use of electroless deposition of metal is an alternate approach to flip-chip bonding.[9–11] The yield strength of the electroless bonding was high enough to successfully bond pillars together; however, defects or voids in the electroless metal between mated pillars is an issue.[12] Trapped voids could be an origin of various failure modes, such as rupture during thermally induced stress, electromigration due to current crowding around the voids, and high-frequency electrical noise. Voids can be created during the joining of pillars due to inadequate plating in the narrow gap between the two pillars surfaces. For example, pillar-to-pillar gaps as wide as 5 to 20 μm may be encountered in flip-chip bonding. The formation of dome-shaped pillars to reduce the initial gap between the two surfaces and the use of a surfactant to stimulate plating in the narrow gap were suggested to improve the bonding process.[13] These actions provide better deposition of the fillet between pillars compared to flat-top pillars with unmodified plating baths.[13] However, there remain fundamental issues in bonding large diameter pillars due to void trapping in the electroless metal joining the pillars. If the deposition rate difference in the gap at the center of the pillars being joined is less than that of the mass transfer preferred region at the edge of the pillars, then voids can be created. Thus, it is highly desirable to control of the deposition rate of the electroless bath to suppress deposition at the spatially favored regions, such as the pillar edge, so as to maintain access to the center of the pillar as the gap is filled. Organic additives can be added to electroless baths to suppress the deposition rate.

Trench filling in geometrically restricted areas has been accomplished in copper electrodeposition through the use of accelerators acting at the bottom of a trench with suppression at the top of the trench. A similar approach was taken in filling through silicon vias (TSV) by use of levelers. It is of interest to extend this concept to electroless copper deposition, such as used to fill trenches and bonding of pillars.

A majority of the literature on copper bottom-up filling is based on the accelerator-suppressor combinations, or suppression-only to cause a favorable deposition rate in the geometrically restricted region. The organic additives used to control the deposition rate include polyethylene glycol (PEG),[14,15] bis-(3-sulfopropyl)-disulfide (SPS),[16,17] similar mercapto or disulfide molecules,[18,19] or their combinations.[20–25] The most widely reported additive is PEG, which can be used to induce bottom-up filling in small trenches. In this case, the inhibition of the deposition rate caused by PEG can affect both the geometrically restricted area (e.g. bottom of the trench) as well as the favored regions (e.g. top of the trench). However, this generally occurs mostly on very small size trenches, less than 1 μm width.[15]

The second approach to bottom-up filling in electroless deposition is based on SPS and similar additives, which contain a thiol and/or disulfide group in the structure. Although the actual mechanism and function as a suppressor or accelerator is still being investigated, these compounds can act as either accelerator or suppressor.[18–21] Most of the work has been focused on the electroless filling of cavities smaller than the 10 to 50 μm deep, and 5 to 10 μm width needed for off-chip structures. The difference between conventional (submicrometer) trench filling and direct Cu-to-Cu pillar joining (of interest in this study) for off-chip interconnection is summarized in Table 1. Currently, there are very few reports which describe the application of Cu electroless plating on the TSV-scale (i.e. 10 to 50 μm). Electroless plating is often considered for seed layer formation.[26] In this paper, the effect of organic additives in Cu electroless bonding was studied with the primary objective being the void-free joining of two dome-shaped, large diameter (50 and 300 μm) pillars. The behavior of the suppressor in terms of deposition rate as a function of mass transfer conditions is reported.

Experimental

Cu pillars with a square base were fabricated by electrodeposition in polymer mold. The pillars were 150 μm tall with a dome-shaped top. The diced chips containing the pillars were aligned and temporarily flip-chip bonded with solder paste or low-temperature melting wax to hold them in place while the electroless fillet of copper was deposited to bond the two components together. Details of the structure are described elsewhere.[12] A variety of pillar shapes and heights were used in the experiments. The most common shape was a 280 μm square-shaped pillar. The pillars had a small height difference caused by non-uniform plating during their fabrication. The height difference was reduced by performing a brief chemical mechanical polishing step before bonding which also gave the pillars a slight dome-shape. The aligned samples were rinsed in 1% sodium dodecyl sulfate (SDS) solution to facilitate filling the liquid inside the gap between the devices. The native Cu oxide on the copper pillars was dissolved and

*Electrochemical Society Student Member.
**Electrochemical Society Fellow.
zE-mail: kohl@gatech.edu

the pillars were cleaned with an aqueous citric acid (3 g/L), H_2O_2 (3 vol.%) immersion for a few minutes. Next, the sample was dipped into Cu electroless deposition solution. The electroless plating bath was composed of $CuSO_4$, EDTA, KOH, HCHO, $K_4Fe(CN)_6$, HCl, MeOH and additives.[12] The samples were mounted on a plastic rotator, and rotated in the bath in a controlled manner so as to provide gentle agitation. The deposition temperature was held at 50°C, and air purging was used to suppress the homogeneous reduction of Cu during the plating.

To analyze the effect of SPS, a set of deposition rate measurement experiments were performed. A Cu coated wafer was made using DC sputtering. The thickness of the metal was 300 nm deposited on 20 nm Ti which acts as an adhesion layer. The copper sample was attached to the rotator and was immersed into the electroless deposition (ELD) bath. After 1 hr of plating, the samples were rinsed and the deposition rate was measured using surface profilometry. The effect of rotating speed and additives on the deposition rate was evaluated.

After deposition, the samples were rinsed in DI water and dried in a nitrogen stream. Then samples were mounted in an acryl polymer mold and polished for cross-sectional examination. The polished samples were dipped in the citric acid-H_2O_2 solution for few minutes to clean the electroless plated layer. The etch rate of the electroless copper is slightly faster than that of electroplated copper due to its smaller grain size.[13] The etch process also reveals the boundary between electroless and electroplated area. Shear testing was performed using an Instron 5820 to measure the bond strength. However, in all cases the bond strength of the electroless copper joining the two pillars was greater than the adhesive strength of the Ti metal onto the substrate so only a lower limit of the pillar-to-pillar bond strength could be obtained.

Results and Discussion

The deposition rate of the ELD copper was first characterized as a function of deposition parameters and additive type. The film thickness after a 1 h deposition was measured as a function of rotation speed of the rotator for three different ELD baths, as shown in Figure 1. Higher rotation speed corresponds to greater mass transfer. The bath containing only Triton X-100, a well-known surfactant sometimes used for bubble suppression, showed a slight decrease in deposition rate up to 100 rpm. The rate decreased to 4.5 μm/hr which

is a 38% decrease from the stagnant solution. This is most likely due to the enhanced oxygen transport to the surface where it can be reduced to water. The reduction process consumes electrons produced from the oxidation of formaldehyde which could otherwise be used to reduce copper ions to copper.[27] This result was confirmed by purging the oxygen from the bath. We note that dissolved oxygen also acts as a stabilizing agent for the bath. Dissolved oxygen inhibits the spontaneous (homogeneous) reduction of copper ions by formaldehyde in the bath. The suppression effect with SPS, Fig. 1, was much greater than that of Triton X-100 only. At 100 rpm rotating speed, the deposition rate dropped to 1.7 μm/hr, a 71.5% decrease in rate. The rate decreased further to 0.94 μm/hr (84.0% decrease) at 300 rpm. This suppression effect is different from the effect of SPS in most electroplating baths because the enhanced mass transfer at high rotation speeds is supposed to help feed reactants to the substrate and increase the limiting current. The suppression of the ELD rate by SPS could be due to the adsorption of SPS and its consumption (or physical presence on the surface) during the electroless process. The concentration of SPS would achieve a steady-state condition on the electrode surface due to the length of time of these experiments (i.e. 1h) and could be lower than the bulk concentration, if it is consumed. However, the high mass transfer coefficient would enhance the transport of SPS to the electrode surface and make its surface concentration closer to the bulk value at high agitation rates. Furthermore, the decrease in the deposition rate would likely decrease the consumption rate of SPS, which would also bring its surface concentration closer to the bulk concentration. This result provides an important piece of information as to the higher deposition rate at lower mass transfer conditions, as one would find in the geometrically restricted areas of pillar-to-pillar bonding and the ability of ELD to produce void-free deposits. That is, the supply of SPS to the edge of the bonded pillars is greater than the supply of SPS to the center of the gap between pillars resulting in preferred ELD plating in the gap.

PEG and SPS can each suppress the electroless deposition process; however, their mechanisms are slightly different. The local suppression by PEG is due to its large molecular weight and slow diffusion to the surface, which provides greater suppression at the entrance to a trench, particularly at the early stages in the deposition process. The diffusion coefficient of PEG-4000 (i.e. 4000 g/mol) is estimated to be around 1/3 of that of the Cu-EDTA complex.[20] This model is appropriate when the trench size is small with respect to the size of PEG and plating at the bottom of the trench is fast and will exceed diffusion of PEG into the void. However, since the molecular size of SPS is smaller than that of the Cu-EDTA complex, its diffusion into the trench is not size restricted. PEG is usually adsorbed without being consumed during the ELD process, whereas SPS is believed to be adsorbed and consumed. PEG has been shown to produce good bottom-up filling behavior on submicron patterns, which take a relatively short time. Here, the ELD of copper between pillars takes a relatively long time and PEG has time to reach a steady state condition, regardless of position on the sample. This assumption is confirmed by the deposition rate data in Fig. 1. It shows that PEG has a lower deposition rate (greater suppression) in the absence of forced convection, compared to SPS, however, forced convection has no effect. Thus, it would be adsorbed on the surface exposed region more quickly than within the trench, and possibly have little or no suppression effect within the trench, for short time depositions.

If the consumption of SPS induces local suppression, the deposition profile should follow the SPS concentration profile. If the SPS concentration is low, then the deposition rate at the entrance to a trench would not be adequately suppressed so as to allow trench filling before the entrance to the trench was pinched off. In the case of pillar-to-pillar bonding, this would result in the void at the center of the pillars. A series of pillar-to-pillar bonding experiments were performed with different SPS concentrations and the results are shown in Figure 2. A low concentration of SPS, 1 mg/L, showed the case of pinching off of the void entrance, Fig. 2a. At the other extreme, at a high concentration of SPS, the deposition was suppressed regardless of the geometric location, even at the center of the pillars. This resulted in a low plating
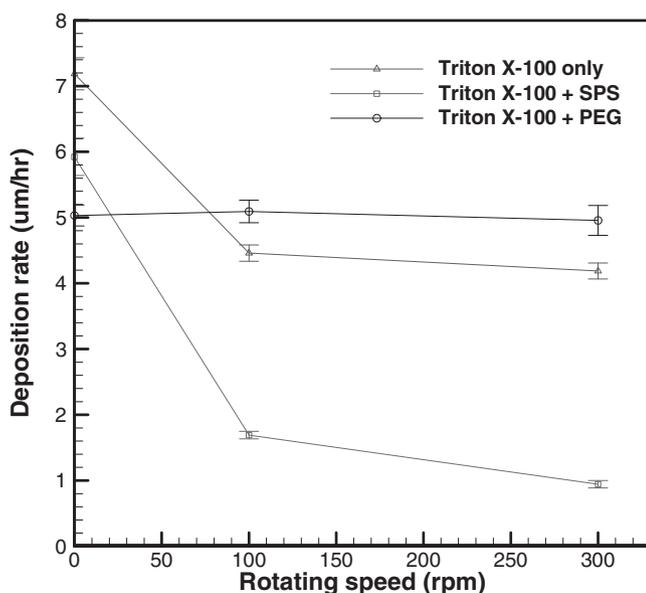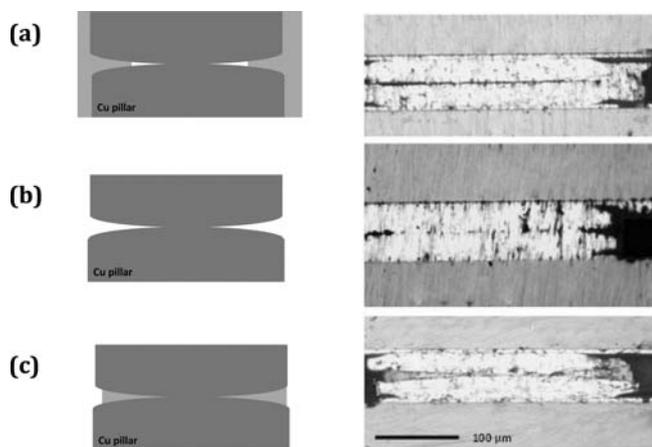

Figure 1. Comparison of the deposition rate of Cu electroless plating according to the addition of additives and the rotating speed of the sample: all of the data were measured after 1 hr of plating.

Figure 2. The joining profile of the two dome-shaped 280 μm circular Cu pillars by electroless plating with the addition of PEG and SPS and their schematic diagrams: (a) gap closing at earlier stage (1 mg/L of SPS), (b) no growth at the center due to strong suppression (3 mg/L) and (c) local suppression at the outside with void-free joining from the center (2 mg/L).

rate everywhere and little differentiation between the entrance to the trench and center of the void between the pillars, Fig. 2b. Thus, a precise concentration of SPS is needed to provide local suppression in geometrically restricted areas to achieve void-free pillar joining. Fig. 2c shows the effect of 2 mg/L SPS. Suppression is observed in the high mass transfer region at the entrance to the gap between pillars while still allowing a higher deposition rate in the restricted area between the pillars resulting in void-free closure of the gap. This is the expected concentration dependency observed in Fig. 1. The ability to preferentially deposit metal in the geometrically restricted area is similar to the result obtained in the bottom-up electroplating of trenches.

The time-dependent growth behavior also showed strong suppression at the outside of the pillar, whereas a higher growth rate was observed at the center. After 1 hr of plating, Cu filled most of the gap area, whereas the outside skin of the pillars showed very low deposition rate. After complete filling of the gap, copper started to grow from the outside of the pillar, making large protrusions toward the outside.

The mechanism of SPS suppression under these conditions is clearly different from the previously reported accelerator function of SPS in acid-copper electroplating. SPS was described as a floating catalyst on the surface of the copper.[28,29] The change in mechanism
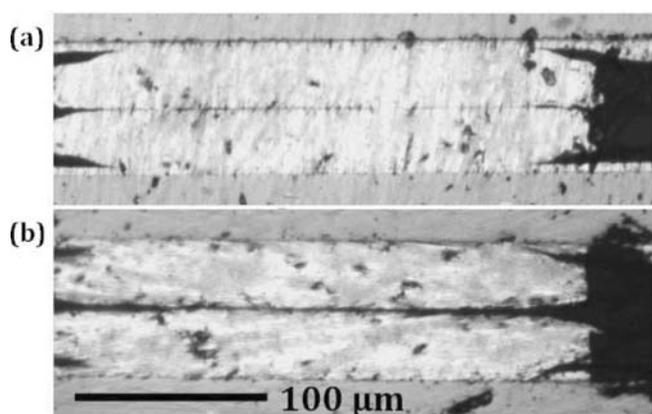
is likely due to the different chemical environment in the two cases. Copper is usually electroplated from an acidic solution at pH around zero, and electroless deposited from a highly alkaline bath containing a complexing ligand, such as EDTA. The acid electroplating baths also contain chloride ions which interact with the Cu surface. The electroless bath is operated at high pH because of the mechanism for formaldehyde oxidation, which consumes hydroxide. Mercapto-carboxylic acids have a similar behavior to SPS in bottom-up ELD trench filling.[19] It is reasonable to conclude that the origin of the local suppression here, at high pH, is due to the adsorption of SPS via the mercapto group, not the sulfonate moiety.

Currently, there is no clear explanation on how SPS is depleted inside the spatially restricted gap in the alkaline electrolyte. Two mechanisms could be considered. First, the SPS molecule can be converted to an inert form on the surface by a chemical or electrochemical reaction. Second, SPS can be incorporated into the film. The incorporation of SPS has been confirmed several times in the literature. Auger electron spectroscopy has been used to show that the concentration of sulfur in the Cu ELD film is 1 to 2 atomic percent when 0.5 to 5.0 mg/L of SPS was added to the bath.[16] It was also observed that the copper resistivity increased with SPS addition to the bath.[16] Inoue et al. reported that sulfur and chloride were detected at the top of the trench (ca. 0.05 wt%) when a bath with 0.1 mg/L of SPS was used. However, these products were not detected at the bottom of a trench (through silicon via), as determined by X-ray fluorescence.[26] These results confirm that a small amount of SPS could be incorporated into the Cu film during the plating process. The first approach is based on the fact that the SPS could be electrochemically reduced to 3-mercapto-1-propanesulfonic acid (MPSA), as shown by Equation 1.[30]

$$SPS + 2e^- \rightarrow 2MPS^- \qquad [1]$$

This reaction would compete with the Cu reduction reaction and decrease the deposition rate. However, both mechanisms could occur simultaneously. The reduced MPSA molecule would be the stronger adsorbate onto the Cu surface and more easily incorporated into the Cu film than SPS, producing a stronger suppression effect. Interestingly, when MPSA was used in place of SPS (at twice the SPS concentration), it showed a much greater degree of suppression than SPS without any useful spatial variation in rate (Fig 3). No growth of Cu was observed regardless of position on the Cu pillar. This result implies that the disulfide group plays an important role in local suppression in geometrically restricted areas. It also suggests that the SPS is not quantitatively reduced to MPSA, Eq. 1, since the equivalent amount of MPSA acts as a stronger suppressor than SPS. This is not surprising since the yield of SPS reduction to MPS via formaldehyde oxidation is not expected to be 100%. One could envision a surface initiated, partial reduction of SPS to MPSA where the concentration of MPSA inside the geometrically restricted region between the pillars was higher than in the bulk of solution because of the higher surface-to-volume ratio of the solution in the region between the pillars.

In addition, 2-mercapto-5-benzimidazolesulfonic acid (MBIS), which has been reported to be functionally similar to SPS in Cu electroless deposition,[31] has shown local suppression and void filling for structures with similar geometry to those used here. The electroless Cu fills the gap between two pillars completely without any seam or void as shown in Figure 4. MBIS has a single thiol group and does not have disulfide bond (like MPSA). It exhibits local-suppression. The exact mechanism of suppression for these compounds is still under investigation and may be the subject of future study.

There could be an equilibrium between SPS and MPS, but in this case, the adsorption of MPS onto the surface could be irreversible due to strong adsorption strength of thiol group. In case of MBIS (which has slightly different molecular structure but has thiol and sulfonate functional groups), though it does not have disulfide bond (like MPSA) we expected that it would not show similar functionality to SPS but interestingly it has local- suppressive performance. That is another interesting aspect and needs deeper review, but one of our
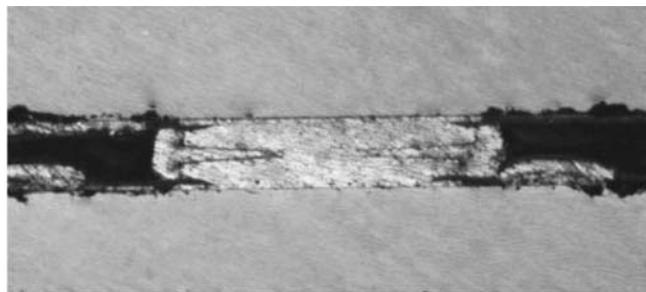

Figure 3. The cross-section of the two dome-shaped Cu pillars after Cu electroless plating with the addition of MPSA: (a) 2 ppm of MPSA + 60 μL/L of Triton X-100, (b) 4 ppm of MPSA + 60 μL/L of Triton X-100. In all cases 280 μm circular pillars were used.

Figure 4. The cross-section of the dome-shaped Cu pillars (280 μm after Cu electroless plating with the addition of MBIS and Triton X-100 (60 μL/L).

assumptions is that the interaction between thiol and Cu surface could be changed due to the overall molecular structure.

The grain structure of the electroless deposited metal used in pillar-to-pillar bonding, prior to annealing, was analyzed by focused ion beam (FIB) sectioning. FIB technique was chosen in order to study the bonding seam region and get comprehensive information of void morphology as opposed to a TEM technique which would give localized information. As shown in Figure 5, Cu filled the space between the two domes. The ELD had a small grain structure and was clearly distinguished from the large grain electroplated pillars. The thickness of the plated metal at the region outside of the gap was less than the thickness of the metal inside the gap due to the suppression effect of the ELD bath. This shows that the pillar-to-pillar bonding had been initiated from the center of the gap.

The total processing time for electroless bonding can be reduced significantly by changing additives in the bath as shown in a previous publication.[10] Currently, the fill process (complete bonding) requires 1.5 to 2 hr for 150 um diameter pillars, and 0.5 to 1 hr for 50 um scale pillars. Compared to Cu bonding, this technology will not require intensive surface preparation steps and mechanical pressing/thermal treatment making it more commercially viable.

In this process, bonding has been carried out on an array of copper pillars; however wafer-level bonding can be carried out using this process. Our primary target is to bond a silicon chip-to-polymer package (which is currently serviced by solder bonding). Therefore we have focused on "single chip-to-single package". We can expect the wafer level bonding to have a higher throughput. Better precision tool system and controlled bath chemistry could be used to first align the wafers in the chamber (with initiating the plating step on the surface) then contact two pillars in the liquid to complete the electroplating.
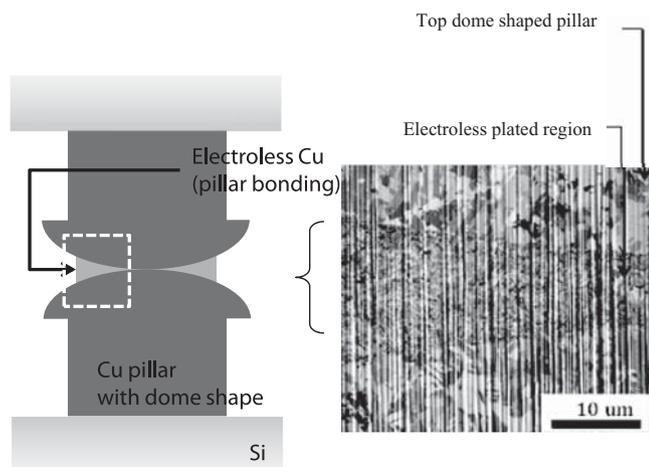
Conclusions

The effect of a suppressor on the electroless deposition of copper in the void-free, Cu-to-Cu electroless joining of copper pillars has been investigated. It has been shown that SPS suppressed the electroless deposition at higher mass transfer resulting in filling of narrow gaps. This filling and suppression behavior is likely due to the consumption of SPS at the Cu surface. This assumption is supported by deposition rate measurements using Cu films. At the optimized concentration of SPS, Cu growth was initiated from the center of the gap (the narrowest part) to the outside, with strong suppression in the outermost region. The FIB analysis confirmed that the direction of growth was clearly from the center to the outside, without any significant void trapping at the center of the gap.

Acknowledgments

References

1. R. R. Tummala, P. M. Raj, A. Aggarwal, G. Mehrotra, S. W. Koh, and S. Bansal, *56th Electronic Components and Technology Conference* 2006.
2. A. Fan, A. Rahman, and R. Reif, *Electrochemical and Solid-State Letters*, **2**(10) 534 (1999).
3. T. H. Kim, M. M. R. Howlader, T. Itoh, and T. Suga, *J. Vac. Sci. Technol.,A*, **21**(2), 449 (2003).
4. C. S. Tan and R. Reif, *Electrochemical and Solid-State Letters*, **8**(6), G147 (2005).
5. E.-J. Jang, S. Hyun, H.-J. Lee, and Y.-B. Park, *Journal of Electronic Materials*, **38**(12), 2449 (2009).
6. P. Gueguen, L. D. Cioccio, P. Gergaud, M. Rivoire, D. Scevola, M. Zussy, A. M. Charvet, L. Bally, D. Lafond, and L. Claveliera, *J. Electrochem. Soc.*, **156**(10), H772 (2009).
7. A. Shigetou and T. Suga, *Proc. 2010 Electron. Comp. and Technol. Conf.*, 872.
8. D. F. Lim, X. F. Ang, J. Wei, C. M. Ng, and C. S. Tan, *Electrochemical and Solid State Letters*, **13**(12), H412 (2010).
9. A. He, T. Osborn, S. A. Bidstrup Allen, and P. A. Kohl, *Electrochemical and Solid-State Letters*, **9**(12), C192 (2006).
10. T. Osborn, A. He, N. Galiba, and P. A. Kohl, *Journal of The Electrochemical Society*, **155**(4), D308 (2008).
11. T. Osborn, N. Galiba, and P. A. Kohl, *Journal of The Electrochemical Society*, **156**(7), D226 (2009).
12. H.-C. Koo, C. Hunter Lightsey, and P. A. Kohl, *IEEE transactions on Components, Packaging and Manufacturing Technology*, accepted.
13. H.-C. Koo, R. Saha, and P. A. Kohl, *J. Electrochem. Soc.*,**158** (12), D698 (2011).
14. M. Hasegawa, N. Yamachika, Y. Shacham-Diamand, Y. Okinaka, and T. Osaka, *Appl. Phys. Lett.*, **90**, 101916 (2007).
15. W. K. Han, G. H. Hwang, S. J. Hong, H. H. An, C. S. Yoon, J. H. Kim, M. J. Lee, G. Hong, K. S. Park, and S. G. Kang, *Material Chemistry and Physics*, **123**, 401 (2010).
16. C. H. Lee, S. C. Lee, and J. J. Kim, *Electrochimica Acta*, **50**, 3563 (2005).
17. C. H. Lee, S. C. Lee and J. J. Kim, *Electrochemical and Solid-State Letters*, **8**(8), C110 (2005).
18. C. H. Lee, S. K. Cho, and J. J. Kim, *Electrochemical and Solid-State Letters*, **8**(11), J27 (2005).
19. Z. Wang, Z. Liu, H. Jiang, and X. W. Wang, *Journal of Vacuum Science and Technology B*, **24**, 803 (2006).
20. Z. Wang, O. Yaegashi, H. Sakaue, T. Takahagi, and S. Shingubara, *Jpn. J. Appl. Phys.*, **43**(10), 7000 (2004).
21. S. Shingubara, Z. Wang, O. Yaegashi, R. Obota, H. Sakaue, and T. Takahagi, *Electrochem. Solid St. Lett.*, **7**(6), C78 (2004).
22. Z. Wang, O. Yaegashi, H. Sakaue, T. Takahagi, and S. Shingubara, *J. Electrochem. Soc.*, **151**, C781 (2004).
23. X. Wang, Z. Yang, N. Li, Z. Liu, Z. Yang, and Z. Wang, *J. Electrochem. Soc.*, **157**, D546 (2010).
24. C. H. Lee, A. R. Kim, H. –C. Koo, and J. J. Kim, *J. Electrochem. Soc.*, **156**, D207 (2009).
25. M. Hasegawa, Y. Okinaka, Y. Shacham-Diamand, and T. Osaka, *Electrochemical and Solid State Letters*, **9**, C138 (2006).
26. F. Inoue, Y. Harada, M. Koyanagi, T. Fukushima, K. Yamamoto, S. Tanaka, Z. Wang, and S. Shingubaraa, *Electrochem. Solid St. Lett.*, **12**, H381 (2009).
27. J. W. M. Jacobs, and J. M. G. Rikken, *Journal of the Electrochemical Society*, **135**, 2822 (1983).
28. T. P. Moffat, D. Wheeler, and D. Josell, *J. Electrochem. Soc.*, **151**(4), C262 (2004).
29. T. P. Moffat, D. Wheeler, M. D. Edelstein, and D. Josell, *IBM Journal of Research and Development*, **49**(1), 19 (2005).
30. I. Volov and A. C. West, *J. Electrochem. Soc.*, **158**(7), D456 (2011).
31. C. H. Lee, A. R. Kim, H.-C. Koo, and J. J. Kim, *J. Electrochem. Soc.*, **156**(6), D207 (2009).

Figure 5. (a) The FIB images of the cross-section of the joining part (before the annealing) and (b) its magnified image.